Vγ5Vδ1 TCR signaling is required to different extents for embryonic versus postnatal development of DETCs

Koichi Sudo[1], Takero Todoroki[1], Yuyo Ka[2] and Kazuhiko Takahara[1,*]

[1]Department of Animal Development and Physiology, Graduate School of Biostudies, Kyoto University, Yoshida-Konoe, Sakyo, Kyoto, Kyoto 606-8501, Japan. [2]Central Institute for Experimental Animals, Kawasaki, Kanagawa 210-0821, Japan.

[*] **Address correspondence to:** Kazuhiko Takahara, Laboratory of Immunobiology, Department of Animal Development and Physiology, Division of Systemic Life Science, Graduate School of Biostudies, Kyoto University, Yoshida-Konoe, Sakyo, Kyoto, Kyoto 606-8501, Japan.

Phone: +81-75-753-4106, Fax: +81-75-753-4112

E-mail: ktakahar@zoo.zool.kyoto-u.ac.jp

Running title: Direct roles of Vγ5Vδ1 TCR in DETCs development

Keywords: γδ T cell, Fetus, Thymus, Epidermis.

Our manuscript consists of a Word file containing the main text and 35 pages, 6 figures, and a PDF containing 7 supplemental figures.

ABSTRACT

γδ T cells expressing Vγ5Vδ1 TCR originally develop in the embryonic thymus and migrate to the epidermis, forming dendritic epidermal T cells (DETCs) throughout life. It is thought that a TCR signal is essential for their development; *e.g.*, lack of TCR signal-transducer ZAP70 significantly decreases DETC numbers. On the other hand, lack of ZAP70 does not affect $V\gamma5V\delta1^+$ T cells in the embryonic thymus; thus, the involvement of TCR signaling remains elusive. Here, we used SKG mice with attenuated TCR signaling rather than gene-knockout mice. In SKG mice, $V\gamma5^+$ T cells showed a marked decrease (10% of wild-type) in adult epidermis; however, there was just a moderate decrease (50% of wild-type) in the embryonic thymus. In early postnatal epidermis in SKG mice, substantial numbers of $V\gamma5^+$ T cells were observed (50% of wild-type). Their activation markers including CD122, a component of the IL-15 receptor indispensable for DETC proliferation, were comparable to those of WT. However, the $V\gamma5^+$ T cells in SKG mice did not proliferate and form DETCs thereafter. Furthermore, in SKG/+ mice, the number of thymic $V\gamma5V\delta1^+$ T cells increased, compared to SKG mice; however, the number of DETCs remained significantly lower than in WT, similar to SKG mice. Our results suggest that signaling *via* Vγ5Vδ1 TCR is indispensable for DETC development, with distinct contributions to embryonic development and postnatal proliferation.

Main Text

INTRODUCTION

γδ T cells are innate type T cells expressing limited elements of the TCR repertoire (1-3). They develop from $CD4^-CD8^-$ double-negative (DN) cells, like conventional αβ T cells. γδ T cells are classified into several subtypes according to their usage of the TCR repertoire. Each subtype migrates into specific peripheral tissues, where they play key roles in preventing infection in the first line of defense, and maintaining homeostasis *via* stress- or immune-surveillance of tissues (4).

Mouse epidermal γδ T cells expressing the Vγ5Vδ1 TCR (3) are the only lymphocytes in the epidermis, and are known as dendritic epidermal T cells (DETCs). They are involved in skin wound healing, carcinogenesis suppression by immune-surveillance, and promoting IgE production against epithelial carcinomas in addition to innate protection (5-9). DETC precursors develop as the first T lymphocytes in the fetal thymus during embryonic day (E) 16-18 (10,11). In development, it is thought that a TCR signal and a co-stimulatory molecule Skint1, a member of the B7 family expressed on thymic epithelial cells, are essential (12). After migration into the epidermis, DETC precursors further proliferate, and subsequently form DETCs, with extensive formation of dendrites throughout life (13). Therefore, DETCs develop stepwise in the embryonic thymus and the epidermis after birth, unlike αβ T cells.

It was reported that γδ T cells are positively selected *via* a TCR signal in the thymus, and acquire the capability of migration and survival in the peripheral tissues in an MHC class I or class II molecule-independent manner (14-16). Since then, the putative non-MHC ligands for γδ TCR have remained elusive. The combination of the Vγ5 TCR and Vδ1 TCR does not seem to be so important for the γδ T cell to localize in the epidermis, because $Vγ5TCR^-$ DETCs or $Vδ1TCR^-$ DETCs still arise in $Vγ5TCR^{-/-}$ and $Vδ1TCR^{-/-}$ mice, respectively (17,18). However, the TCR signal is thought to be involved in DETC development, based on knockout mice lacking TCR-proximal tyrosine kinases; *e.g.,* $ZAP70^{-/-}$ mice, which show a decrease in DETC numbers, with imperfect dendrite formations in the epidermis (19,20). Another group reported that almost all $Vγ5TCR^+$ cells disappeared in the embryonic thymus in ZAP70 and Syk double-knockout mice; however, the cell numbers seemed to be normal in ZAP70 single-knockout mice (21).These results

suggest a possible involvement of TCR signaling in DETC formation, but the mechanism is still unclear. It is thought that Skint1 upregulates Vγ5Vδ1 TCR signaling for maturation of DETC precursors (22). A Skint1 mutation leads to the impairment of DETCs in the epidermis, partly due to decreased expression of chemokine receptors and a set of TCR-associated molecules; however, it is unclear whether Skint1 directly regulates their respective gene expression and subsequent DETC maturation (22,23). In addition, it has been thought that Vγ5Vδ1 TCR signaling aided by Skint1 is necessary for DETC development, but this hypothesis has not been directly confirmed. Furthermore, a functional replacement/change of kinases is possible in the kinase-knockout mice. For example, it was reported that T cells from ZAP70-deficient patients upregulate Syk expression, resulting in replacement of the TCR signal molecule complex (24-26); in some systemic lupus erythematosus patients, the TCR complex changes from CD3ζ and ZAP70 to FcεRIγ and Syk. (27,28). These results highlight the difficulty of interpretating experiments using gene-knockout mice for the investigation of $V\gamma5V\delta1^+$ T cell/DETC development.

To further identify relevant roles of Vγ5Vδ1 TCR signaling in DETC development, we utilized SKG mice with a spontaneous ZAP70 mutation (29) rather than gene-knockout mice. ZAP70 is the TCR-proximal tyrosine kinase binding to the immunoreceptor tyrosine-based activation motif (ITAM) of the TCR complex, and it phosphorylates associated molecules to transduce the TCR signal onward. The mutation of ZAP70 in SKG mice reduces its binding affinity to the TCR complex, resulting in attenuation of the TCR signal (29). Despite the attenuated TCR signaling, SKG thymocytes and T cells express levels of ZAP70 and Syk proteins comparable to those of wild-type (WT) mice (29). Wencker *et al.* reported a decrease of $IL\text{-}17^+$ γδ T cells without a change in the overall number of γδ T cells in the SKG mouse thymus (30), suggesting the suitability of the mice for analyses of γδ T cell development. Accordingly, we considered that the SKG mice would be particularly amenable to elucidate the relevant involvement of Vγ5Vδ1 TCR signaling in DETC development during the fetal and postnatal stage.

METHODS

Mice

BALB/c mice were obtained from Japan SLC (Hamamatsu, Shizuoka, Japan) and CLEA Japan, Inc (Meguro, Tokyo, Japan). SKG mice were obtained from Dr. Sakaguchi (Osaka University, Osaka, Japan). Mice were maintained under specific pathogen-free conditions with verification every three months, and they were used at 8-12 weeks of age unless otherwise stated. To obtain timed pregnancies, mice were mated overnight, and E0 was defined as the day that the vaginal plug was discovered. All experiments were conducted according to our institutional guidelines.

Reagents and antibodies

Anti-Vγ5Vδ1 TCR (17D1) was a generous gift from Dr. Robert E. Tigelaar (Yale University, School of Medicine, CN, USA). Antibodies to murine CD3ε (17A2), CD4 (RM4-5), CD25 (PC61), CD100 (BMA-12), CD122 (5H4), IFN-γ (XMG1.2), IL-17A (TC11-18H10.1), JAML (4E10), Langerin (4C7), Syk (5F5), T-bet (4B10), β TCR (H57-597), γδ TCR (GL3), Vγ5 TCR (536) and fluorochrome-labeled streptavidins were purchased from BioLegend (CA, USA). Anti-murine Ly6c (ER-MP20) antibodies were purchased from BMA Biomedicals (Augst, Switzerland). Antibodies to murine CD3ε (145-2C11), CD4 (GK1.5), CD5 (53-7.3), CD11b (M1/70), CD11c (N418), CD27 (LG.7F9), CD44 (IM7), CD45 (30-F11), CD69 (H1.2F3), NKG2D (CX5), Rorγt (AFKJS-9) and 7AAD were purchased from eBioscience (CA, USA). Antibodies to murine B220 (RA3-682), CD4 (GK1.5), CD8α (53-6.7), CD11b (M1/70), CD11c (HL3), CD24 (M1/69), CD45RB (16A), Gr-1 (RB6-8C5), I-A^d (10-3-4), I-A^d (AMS-32.1), β TCR (H57-597), γδ TCR (GL3), Annexin V, anti-human Ki-67 (B56), anti-human Stat5 (pY694) (47/Stat5 (pY694)) and mouse IgG1 κ were purchased from BD Pharmingen (NJ, USA). Antibodies to rat IgM μ chain were purchased from Jackson ImmunoResearch (PA, USA). UEA-I was purchased from Vector Laboratories (CA, USA). A LIVE/DEAD Fixable Near-IR Dead Cell Stain Kit was purchased from Thermo Fisher Scientific (MA, USA).

Cell preparation

Ears were separated into dorsal and ventral halves. Both sides of the ear skin were incubated with at least 1.0×10^5 BAEE unit/ml trypsin (Sigma-Aldrich, MO, USA) in Hanks' balanced salt solution (HBSS) without Ca^{2+} and Mg^{2+} for 60 min at 37ºC, followed by separation into dermis and epidermis. Epidermis was cut into pieces and treated with RPMI1640 containing 5,000 U/ml DNase I (Sigma-Aldrich) for 60 min at 37ºC. The tissue suspension was passed through a stainless steel mesh and cells were pelleted by centrifugation. The pellet was resuspended in RPMI1640 containing 10 mM EDTA to disrupt cell aggregation. Immediately after dissection, fetal thymus was treated with PBS containing 0.125% trypsin-EDTA (Sigma-Aldrich) without Ca^{2+} and Mg^{2+} for 30 min at 37ºC, then teased with a 22-gauge needle. Red blood cells were removed from the tissue cells with ACK lysis buffer (150 mM NH_4Cl, 1 mM $KHCO_3$ and 0.001 mM EDTA). The cells were passed through a stainless steel mesh and 35 μm pore size nylon mesh to obtain a single cell suspension.

Flow cytometry and cell sorting

Fc receptors on cells were blocked with an anti-CD16/32 mAb in staining buffer (1% FCS, 0.02% NaN_3, 5 mM EDTA in PBS) for 15 min on ice, then stained for 30 min on ice with mAbs, as indicated. Net MFI was obtained by subtraction of the isotype mAb MFI from that of the specific mAb. 17D1 hybridoma culture supernatant was diluted 5- to 10-fold and used as a primary mAb, followed by staining with anti-rat IgM antibody. Annexin V staining was performed in Annexin V binding buffer (140 mM NaCl, 2.5 mM $CaCl_2$, 10 mM HEPES) for 15 min at room temperature after cell surface staining. For intracellular staining, cells were fixed and permeabilized with a BD Cytofix/Cytoperm Fixation/Permeabilization Kit (BD Biosciences) for 20 min on ice and stained with fluorophore-conjugated antibodies for 30 min at room temperature. For pSTAT5 staining, stimulated cells were fixed with BD Phosflow Lyse/Fix Buffer (BD Biosciences) for 10 min at 37ºC, and then permeabilized with BD Phosflow Perm Buffer III (BD Biosciences) for 30 min on ice according to the manufacturer's protocol. The cells were stained with fluorophore-conjugated

anti-pSTAT5 antibody for 30 min at room temperature. Data were collected on FACSCalibur or FACSAria III systems and analyzed with FlowJo v10 (BD Biosciences, NJ).

Immunostaining of epidermal sheets and thymus sections

Thymuses were frozen in Tissue-Tek OCT-compound (SAKURA SEIKI, Tokyo, Japan) at -20ºC. Cryosections (7 μm in thickness) were dried and stored at -80ºC until immunostaining. The sections were fixed in acetone for 20 min at room temperature and then dried again. After Fc blocking with an anti-CD16/32 mAb for 60 min at 4ºC, sections were stained with antibodies in staining buffer for 90 min at 4ºC. Epidermal sheets were prepared from the dorsal side of ear skin. Briefly, ears were treated with hair removal cream and separated into dorsal and ventral halves; the dorsal sheets were immersed in 0.5 M ammonium thiocyanate (Wako, Osaka, Japan) for 60 min at 37ºC, and the epidermis was then separated from the dermis. The epidermis was fixed with acetone for 20 min at room temperature and, after Fc blocking, stained overnight at 4ºC with antibodies in staining buffer. Samples were washed with PBS and stained with Cy3-labeled streptavidin for 30 min at 4ºC. Images were obtained using a fluorescence microscope BX51 (OLYMPUS, Tokyo, Japan) and imaging software (SlideBook; Intelligent Imaging Innovations, CO, USA).

Thymocyte culture

Thymocytes (2×10^5 cells) from E18 fetuses were cultured in 200 μl/well complete RPMI1640 medium (cRPMI) containing 10% FBS, 50 μM 2-mercaptoethanol, 2 mM L-glutamine, 100 U/ml penicillin and 100 μg/ml streptomycin with or without 50 ng/ml recombinant IL-15 (PeproTech, NJ, USA) in a 96-well flat-bottom plate for 48 hours at 37ºC. For the analysis of STAT5 phosphorylation, thymocytes (2×10^5 cells) from E18 fetuses were stained with cell surface marker -specific antibodies and cultured in 200 μl/well pre-warmed cRPMI with or without 50 ng/ml recombinant IL-15 in a 96-well flat-bottom plate for 15 min at 37ºC. The cells were fixed and permeabilized with BD Phosflow Lyse/Fix Buffer and BD Phosflow Perm Buffer III according to

the manufacturer's protocol. For intracellular staining of IFN-γ and IL-17A, thymocytes were stimulated with 25 ng/ml phorbol 12-myristate 13-acetate (PMA), 1 μg/ml ionomycin and 1 μl/ml GolgiPlug for 4 hours at 37ºC.

RNA isolation and qRT-PCR

Total RNA was extracted from thymocytes and epidermal cells using TRIZOL (Thermo Fisher Scientific). Total RNA was extracted from thymic Vγ5Vδ1$^+$ T cells using RNeasy Mini Kit (Qiagen, Hilden, Germany). Amplification of genes of interest and the housekeeping gene (*β-actin*) was performed using a BRYT Green dye assay with GoTaq 1-Step RT-qPCR System (Promega, WI, USA) and a StepOnePlus Real-Time PCR System (Applied Biosystems, CA, USA). Expression was calculated with the $\Delta\Delta C_T$ method normalized to *β-actin*. The following primers were used: *β-actin*: forward 5'-AGCCTTCCTTCTTGGGTATGG-3', reverse 5'-TGTGTTGGCA TAGAGGTCTTTACG-3'; *Car*: forward 5'-CGTTCTTGTTAAGCCTTCAGGTACA-3', reverse 5'-CAACGTCTAGTCGCAGCATACAC-3'; *H60c*: forward 5'-GACAGAGACAGGGTGAAG ATGCT-3', reverse 5'-AGCATGATGAGTCATATGTTGAGGAT-3'; *Il-15*: forward 5'-GGAA TACATCCATCTCGTGCTACTT-3', reverse 5'-CCTACACTGACACAGCCCAAAA-3'; *Il-15rα*: forward 5'-GCTATGGAGTCCAGGCCATT-3', reverse 5'-GCTAGGGAGGGGTCTCTG AT-3'; *Jak1*: forward 5'-CCTTCTTTGAGGCTGCTAGCA-3', reverse 5'-CTTCCACCATGAT ATTTTCCACATC-3'; *Jak3*: forward 5'-ACCCAAGGAAAAGTCCAATTTG-3', reverse 5'-AT TGTGTGGAAGCTCAGCTGTGT-3'; *PlexinB2*: forward 5'-CACTTCTGCAGAGTATGGTTC TATCC-3', reverse 5'-GGAGCCGGAACACCTTGTC-3'; *Skint1*: forward 5'-AGAGGTCAAG ATCACAGCCATAAAC-3', reverse 5'-GAACCAACCTCCAGAGTGACACT-3'; *Stat5a*: forward 5'-AGAAACATGTCACTGAAAAGAATCAAG-3', reverse 5'-CTGCCAACGCTGAA CTGAGA-3'; *Stat5b*: forward 5'-GAGAACACCCGCAATGATTACA-3', reverse 5'-GTCAGA CCTCTTGATTCGTTTCAG-3'; *Tgf-β*: forward 5'-GCTGAACCAAGGAGACGGAAT-3', reverse 5'-GCTGATCCCGTTGATTTCCA-3'.

16S rRNA sequencing

Whole ears were harvested and stored at -80 ºC until use. DNA isolation from the samples and 16S rRNA sequencing were performed by Bioengineering Lab (Kanagawa, Japan). Briefly, the samples were disrupted mechanically, and DNA was isolated using an MPure Bacterial DNA Extraction Kit (MP Biomedicals, CA, USA). The V1/V2 region of 16S rRNA was amplified with modified-27F and modified-338R primers. The amplicons were purified and subjected to secondary PCR with primers containing index sequences, followed by purification. Libraries were sequenced on an Illumina MiSeq system with 2 × 300 bp pair-end reads using MiSeq Reagent Kit v3 (Illumina, CA, USA). Raw sequencing data were processed with QIIME2 pipelines followed by denoising with DADA2 (31). Taxonomy was assigned to amplicon sequence variants (ASVs) using a feature-classifier against the Greengene 13_8 97% OTU reference sequences. The alpha-diversity index and beta-diversity analyses were calculated with Shannon index and unweighted UniFrac, respectively. Skin microbiota were characterized by calculating a linear discriminant analysis (LDA) score with LEfSe version 1.0 in the Huttenhower lab Galaxy server (32).

Data availability

The accession number for the raw data of 16s rRNA sequencing in this paper is NCBI Bioproject: PRJNA786442.

Statistical analysis

Data are expressed as the mean ± S.D. Statistical significance was determined by a two-tailed Student's *t*-test. Statistical significance in LEfSe analysis was determined by A Kruskal-Wallis test and a pairwise Wilcoxon test. Statistical significance in α-diversity index was determined by Kruskal-Wallis test. All experiments were performed two or more times, and representative results are shown.

RESULTS

Attenuated TCR signaling impairs DETC formation.

We first checked ear epidermis of adult mice by flow cytometry, observing that the number of DETCs was significantly lower in SKG mice than in WT mice **(Fig. 1A and Fig. S1A)**. The number of pan-γδ T cells was also significantly lower in SKG mice than in WT mice, whereas almost all of the pan-γδ T cells were Vγ5TCR$^+$ cells in both WT and SKG mice **(Fig. S1B and C)**, suggesting that the SKG mutation does not perturb the γδ TCR repertoire, but instead suppresses DETC development. The number of Langerhans cells (LCs), another major type of epidermal immune cell, was comparable between SKG and WT mice, whereas higher expression of Langerin was observed in LCs in SKG than in WT mice **(Fig. 1B and Fig. S1D)**. Epidermal *Tgf-β* mRNA expression, which augments Langerin expression (33), was comparable between WT and SKG mice **(Fig. S1E)**. In immunofluorescence staining of the epidermis, CD3ε$^+$Vγ5TCR$^+$ DETCs appeared to be sparser, with fewer dendrites in SKG mice than in WT **(Fig. 1C and D)**. It was reported that CD103, an integrin subunit of αEβ7, is involved in dendrite formation in DETCs (34); however, the expression level of CD103 on DETCs in WT and SKG mice was comparable **(Fig. 1E)**, suggesting that expression of CD103 is insufficient to generate dendrites, and adequate TCR signaling is necessary for proper dendrite formation. DETCs did not express JAML, CD100 and NKG2D, which are involved in tissue homeostasis and repair **(Fig. 1F)** (35-37), whereas expression of mRNAs for their ligands, *Car* (*Coxsackie and adenovirus receptor*), *PlexinB2* and *H60c* were comparable in WT and SKG mice **(Fig. S1F)**. Consistent with a previous study using TCR δ chain knockout mice (38), the number of epidermal αβTCR$^+$ cells increased in SKG mice **(Fig. S1G)**. These results suggest that appropriate TCR signaling plays important roles in the development of Vγ5TCR$^+$ DETCs in the adult epidermis.

Attenuated TCR signaling impairs the development of Vγ5Vδ1$^+$ T cells in the fetal thymus.

DETC precursors originate in the fetal thymus (10). At embryonic day 16 (E16), the number of DN cells in each stage (DN1-DN4), except for DN3 cells, was comparable between WT and SKG mice **(Fig. 2A and Fig. S2A)**. The number of DN3 cells was slightly lower in SKG mice than in

WT mice **(Fig. 2A; *p* = 0.018)**. To detect Vγ5Vδ1$^+$ T cells, we used a 17D1 monoclonal antibody (mAb) that recognizes the Vγ5Vδ1 TCR epitope (17,39). At both E16 and E18, the number of Vγ5Vδ1$^+$ T cells (identified as Vγ5TCR$^+$17D1$^+$ cells) in SKG mice was approximately half that of WT **(Fig. 2B)**, whereas the number of 17D1$^-$Vγ5$^+$ T cells was lower in SKG mice than in WT mice at E18, but not at E16 **(Fig. S2B and C)**. In E18 thymus, the ratio of 17D1$^+$ cells to pan-Vγ5$^+$ T cells in the thymus was comparable between WT (53.3±4.3%) and SKG (49.4±6.3%) mice **(Fig. S2C)**. These results suggest that the SKG mutation does not affect the balance of Vγ5$^+$Vδ1$^+$ and Vγ5$^+$Vδ1$^-$ γδ T cells, at least during their differentiation in the thymus. The total number of γδ T cells showed a deficit in SKG fetal thymus at E18, but the numbers were comparable in adult thymus in both SKG and WT mice **(Fig. S2D and E)**, as reported previously (30).

At E16, SKG mouse Vγ5Vδ1$^+$ T cells showed surface expression of CD3ε, γδ TCR and Vγ5 TCR was comparable to that of WT mice **(Fig. S3A)**. However, at E18, the respective expression levels on SKG Vγ5Vδ1$^+$ T cells were reduced in comparison with WT mice **(Fig. 2C)**. Expression levels of those molecules on 17D1$^-$Vγ5$^+$ T cells were comparable in both WT and SKG mice **(Fig. S3B)**, suggesting a lower dependency of the cells on TCR signaling. We next checked the localization of Vγ5$^+$ T cells in the fetal thymus of SKG mice by immunofluorescence staining; this showed normal distribution in the UEA-I$^+$ medullary area **(Fig. 2D)**, as previously reported (40). The frequency of Vγ5$^+$ T cell apoptosis including Vγ5Vδ1$^+$ T cells was comparable between WT and SKG mice **(Fig. 2E and Fig. S3C)**. However, Ki-67 staining indicated that there was less proliferation in Vγ5Vδ1$^+$ T cells in SKG mice than in WT mice **(Fig. 2F and Fig. S3D)**, suggesting that adequate TCR signaling is necessary for efficient Vγ5Vδ1$^+$ T cell proliferation, but not for survival. This is unlike αβ T cell positive selection inducing T cell death with insufficient TCR affinity to the antigen-MHC complex **(Fig. S3E)** (29,41,42). We then crossed WT and SKG mice, and evaluated the effect of graded TCR signaling in the development of Vγ5Vδ1$^+$ T cells in the fetus (SKG/+ mice, hereafter). The number of thymic Vγ5Vδ1$^+$ T cells in SKG/+ mice was slightly lower, but not significantly lower, than that of WT mice **(Fig. 2G)**, suggesting that in heterozygotes, the contribution of TCR signaling *via* ZAP70 from the WT allele plus signaling from the SKG mutation is sufficient for the development of Vγ5Vδ1$^+$ T cells in the embryonic thymus. Taken

together, these results suggest that the SKG mutation affects TCR-CD3ε complex expression and proliferation of Vγ5Vδ1$^+$ T cells in the fetal thymus.

Attenuated TCR signaling impairs maturation of Vγ5Vδ1$^+$ T cells in the fetal thymus.

To confirm that attenuated TCR signaling and lower expression of TCR-associated molecules influence Vγ5Vδ1$^+$ T cell representation in the thymus, we first assessed the expression of CD5, an indicator of TCR signal strength (43). At E16, all Vγ5Vδ1$^+$ T cells from WT and SKG mice expressed CD5, but the expression level in SKG mice was lower than that in WT mice **(Fig. 3A)**. At E18, the CD5 expression level on Vγ5Vδ1$^+$ T cells was comparable between WT and SKG mice; however, the frequency of CD5$^+$ cells was slightly lower in SKG mice ($p = 0.017$) **(Fig. 3B)**. The change in the CD5 expression level on 17D1$^-$Vγ5$^+$ T cells was different from Vγ5Vδ1$^+$ T cells, although in both cell types the level was lower in SKG mice than in WT **(Fig. S4A and B)**. These results suggest that, based on CD5 expression, the SKG mutation affects 17D1$^+$ and 17D1$^-$Vγ5$^+$ T cells. On the other hand, it is known that Skint1, a costimulatory molecule, is indispensable for Vγ5Vδ1$^+$ T cell development in the fetal thymus (22). As expected, the expression of *Skint1* mRNA was comparable between fetal WT and SKG mouse thymus **(Fig. S5A)**.

We next examined the effects of an attenuated TCR signal on the expression of maturation markers, CD24, CD45RB and CD122 in Vγ5Vδ1$^+$ T cells (22,44). At E16, frequencies of cells positive for the markers were comparable in WT and SKG mice **(Fig. 3C)**. At E18, frequencies of CD24$^-$ and CD45RB$^+$ cells were comparable in WT and SKG mice; however, CD122$^+$ cell frequency was significantly decreased by the SKG mutation **(Fig. 3D)**. The defects in maturation of 17D1$^-$Vγ5$^+$ T cells seem similar to those of Vγ5Vδ1$^+$ T cells in SKG mice **(Fig. S4C and D)**. CD122, a β subunit of the IL-2 receptor and IL-15 receptor, is induced upon T cell activation *via* the TCR (45). The combination of CD122 and IL-15, rather than IL-2, is necessary for proliferation of Vγ5$^+$ T cells (46,47). Hence, we checked the responsiveness of Vγ5Vδ1$^+$ T cells in the fetal thymocytes to IL-15, showing their lower proliferation in SKG than in WT mice **(Fig. 3E)**. In addition, the stimulated proliferation of Vγ5Vδ1$^+$ T cells by IL-15 treatment of thymocytes, as

determined by the fold change in Vγ5Vδ1$^+$ T cell numbers between E18 cells and cells cultured for 48 hours was significantly impaired in SKG mice, compared to WT mice **(Fig. 3F)**. We also observed hypo-phosphorylation of STAT5, a downstream molecule of the IL-15 receptor (48), in Vγ5Vδ1$^+$ T cells upon IL-15 stimulation in SKG mice **(Fig. 3G)**. On the other hand, the mRNA expression levels of *Jak1*, *Jak3*, *Stat5a* and *Stat5b* in Vγ5Vδ1$^+$ T cells were comparable in WT and SKG mice **(Fig. S5B)**. Thymic expression of *Il-15* and *Il-15rα* mRNA was comparable between fetal WT and SKG mice **(Fig. S5C and D)**. Therefore, these results suggest that the SKG mutation negatively affects expression of CD122, leading to low responsiveness of Vγ5Vδ1$^+$ T cells to IL-15 and hypo-phosphorylation of STAT5.

Attenuated TCR signaling does not affect the cytokine production capacity of Vγ5Vδ1$^+$ T cells.

Previous studies suggested that augmented Syk expression supports TCR signaling in ZAP70-deficint patients (24-26). The expression level of Syk in Vγ5Vδ1$^+$ T cells was comparable between WT and SKG mice **(Fig. 4A)**, thus excluding the possibility that abnormal Syk expression compensates for the SKG mutation in the development of Vγ5Vδ1$^+$ T cells.

We then explored the effect of the SKG mutation on the function of Vγ5Vδ1$^+$ T cells. We first assessed CD27 expression, a well-known marker discriminating γδ T cells producing IFN-γ or IL-17 (49). Almost all of the Vγ5Vδ1$^+$ T cells expressed CD27 in both WT and SKG mice **(Fig. 4B)**. Next, we assessed some informative transcription factors, observing that a high proportion of Vγ5Vδ1$^+$ T cells expressed Rorγt in WT mice, although this transcription factor is known to be characteristic of IL-17-producing T cells **(Fig. 4C)** (50). Vγ5Vδ1$^+$ T cells in SKG mice expressed comparable levels of Rorγt or T-bet to those in WT mice, whereas the number of Rorγt$^+$T-bet$^+$ cells was slightly decreased in SKG mice **(Fig. 4C)**. We observed no mRNA expression of *Sox13* in thymic Vγ5Vδ1$^+$ T cells in both WT and SKG mice at E18 (data not shown). Lastly, we checked the ability of Vγ5Vδ1$^+$ T cells to produce cytokines upon stimulation with PMA and ionomycin. The number of cells producing IL-17 or IFN-γ were comparable in WT and SKG mice **(Fig. 4D)**.

These results suggest that the SKG mutation affects the development of Vγ5Vδ1$^+$ T cells rather than their function, at least with regard to IL-17/IFN-γ production.

Attenuated TCR signaling impairs proliferation of DETCs in early-life mice.

The SKG mutation affects Vγ5Vδ1$^+$ T cell development in the fetal thymus. However, the effects seem to be mild in comparison with the decrease of DETCs in the adult skin; *i.e.*, SKG mice showed about half the number of thymic Vγ5Vδ1$^+$ T cells, but a more severe decrease (about 90%) in adult DETCs compared to WT mice. It is known that, after egress from the fetal thymus, Vγ5Vδ1$^+$ T cells appear in the epidermis, and they start to proliferate 1-2 weeks after birth (13). We therefore checked epidermal Vγ5$^+$ T cells in early-life (16-19-days-old), young (4-weeks-old) and adult (7-weeks-old) mice. In the early-life period, SKG mice showed about half the number of Vγ5$^+$ T cells as WT mice **(Fig. 5A)**. Their activation markers, including CD122, were comparable on Vγ5$^+$ T cells in WT and SKG mice in this period **(Fig. 5B and Fig. S6A)**. However, in the young and adult period, the number of Vγ5$^+$ T cells in SKG mice was significantly lower than that in WT mice **(Fig. 5C and D)**. We also checked these results by immunofluorescence staining, observing substantial amounts of Vγ5TCR$^+$ cells in early-life SKG mice **(Fig. 5E)**. As previously reported (13), Vγ5$^+$ T cells of WT mice had a round morphology during the early-life period, then formed dendrites in the young period **(Fig. 5E)**. However, Vγ5$^+$ T cells in SKG mice showed poor dendrite formation even in the young period **(Fig. 5E)**. In the epidermis in early life, but not in adults, Vγ5$^+$ T cells expressed Syk in both WT and SKG mice **(Fig. 5F)**. However, the frequency of Syk$^+$ cells was lower in WT mice than in SKG mice in early life. These results suggest that the SKG mutation does not lead to upregulated Syk expression to compensate for defective TCR signaling in Vγ5Vδ1$^+$ T cells/DETCs in SKG mice. It was reported that DETCs constitutively engage Skint1 in the epidermis (51), suggesting an involvement of co-stimulation in their proliferation. However, *Skint1* mRNA expression in SKG mouse epidermis was normal **(Fig. S6B)**. Furthermore, *IL-15* and *IL-15rα* mRNA expression levels in the early-life epidermis of SKG mice were in the normal range **(Fig. S6B)**. We then checked the number of DETCs in SKG/+ mice. Unlike in the thymus, the number of epidermal Vγ5$^+$ T cells significantly decreased in SKG/+ mice, to as few as that in SKG mice **(Fig. 5G)**. These results suggest that TCR signaling from ZAP70 from one WT allele plus the SKG allele is not sufficient for the development of DETCs. Taken

together, these results suggest that, in the epidermis, Vγ5Vδ1$^+$ T cells do not properly proliferate because of inadequate TCR signaling, leading to a severe deficiency of DETCs in adult SKG mice.

DETCs develop normally in germ-free conditions.

The SKG mutation induces spontaneous arthritis (29,50). It is thought that this is partly due to the abnormal response of T cells to intestinal microbiota because the arthritis is not induced in SKG mice housed under SPF conditions unless they are treated with β-glucan, a fungal component. Furthermore, β-glucan cannot induce the arthritis by itself in germ-free conditions (53,54). These results imply the presence of abnormal intestinal microbiota in SKG mice. Thus, we hypothesized that the SKG mutation altered skin microbiota, affecting the DETC development. We analyzed skin microbiota by 16S rRNA sequencing and observed that the microbiota were more enriched in SKG mouse skin, whereas the microbial composition, meaning overall species representation, was not different between WT and SKG mice **(Fig. 6A and Fig. S7)**. Interestingly, *Actinomycetales* was less abundant, whereas *Lactobacillaceae*, *Rikenellaceae* and *Lachnospiraceae* were more enriched in SKG mice compared with WT mice **(Fig. 6B)**. These results suggest that the SKG mutation affects skin microbiota. It is also reported that skin microbiota affects IL-17-producing γδ T cells and mucosal associated invariant T (MAIT) cell population in the dermis (55,56). We therefore checked epidermal Vγ5$^+$ T cells in germ-free (GF) mice, observing comparable numbers and a similar morphology to Vγ5$^+$ T cells in SPF mice **(Fig. 6C and D)**. These results exclude the possibility that normal microbiota effect DETC formation. <u>However, we cannot exclude the possibility that the abnormal skin microbiota in SKG mice affects the DETC development.</u>

DISCUSSION

Vγ5Vδ1$^+$ T cells develop in the fetal thymus and proliferate in the epidermis. It is indirectly thought that Vγ5Vδ1$^+$TCR signaling is involved in both these stages; however, the details have remained unclear. In this study, using SKG mice, we showed that appropriate TCR signaling affects in these stages. In SKG mice, attenuated TCR signaling showed more severe defects in the epidermal than in the fetal thymic development of Vγ5Vδ1$^+$ T cells. At present, it is unclear whether the downregulation of TCR signaling by the SKG mutation affects the repertoire of Vδ chain usage, inducing Vγ5$^+$Vδ1$^-$ γδ T cells, as was observed in the epidermis of Vδ1KO mice (18), because we could not detect epidermal Vγ5Vδ1$^+$ T cells using the 17D1 mAb (data not shown).

Previous studies using gene-knockout mice reported that ZAP70 was involved in DETC formation in the epidermis, but not Vγ5$^+$ T cell development in the fetal thymus (19-21). In these reports, DETCs decreased by 50% in ZAP70$^{-/-}$ mice compared with WT mice (19,20). This finding is controversial because the SKG mutation with partial ZAP70 function led to more severe defects in DETCs, relative to those in ZAP70 gene-knockout mice. Several explanations are worth considering. One possibility could involve the mouse background. In these experiments, SKG and ZAP70$^{-/-}$ mice were used in BALB/c and C57BL/6 backgrounds, respectively.

The conflicting results could possibly be explained by usage of kinases in the thymus and in the periphery. αβ T cell thymocytes express Syk in addition to ZAP70, and their Syk expression is downregulated in peripheral T cells (57). While mice with a knockout of either Syk or ZAP70 seem to show no perturbation of DP development, mice with a double knockout show impaired development of DP cells (58-61). Moreover, in ZAP70 knockout mice, the forced expression of Syk restores the development of CD4SP and CD8SP cells (62), suggesting that the two tyrosine kinases have overlapping functions in αβ T cell development. γδ T cells also express both Syk and ZAP70 in the thymus, and their Syk expression is downregulated in the periphery; *e.g.*, in the intestine (39) and the epidermis (Fig. 4A and 5F). However, γδ T cells seem to depend on Syk more than ZAP70, since Syk$^{-/-}$, but not ZAP70$^{-/-}$, mice show decreased numbers of γδ T cells in the embryonic thymus (21). Taking these into consideration, it is possible that Syk is mainly involved or collaborates with ZAP70 in thymic Vγ5Vδ1$^+$ T cell development, and can partially compensate for the insufficient function of mutated ZAP70. In contrast, in the epidermis, Syk

expression is downregulated, and ZAP70 becomes the main kinase involved in DETC proliferation; thus, mutated ZAP70 leads to impaired proliferation. Further study is necessary to identify any distinct contributions of the two tyrosine kinases in Vγ5Vδ1$^+$ T cell development in the thymus and in the periphery.

The expression of Langerin in LCs was upregulated in SKG mice despite a comparable level of *Tgf-β*. Human LCs recognize some ligands, such as HIV1 gp120, β-glucan and wall teichoic acid, *via* Langerin (61-63). It is possible that perturbed microbiota affects Langerin expression in SKG mice (see Fig. 6A, B). In addition, we do not exclude the possibility that DETCs directly control the LC phenotype because some DETCs associate with LCs, and highly polarized TCRs are observed in the contact interfaces (64), albeit the detailed effect is unknown.

Expression levels of TCR-associated molecules on thymic Vγ5Vδ1$^+$ T cells were lower in SKG mice than in WT mice at E18 but not at E16 (Fig. 1C and Fig. S3A). It is conceivable that, in WT mice, the TCR-associated molecules are upregulated from E16 to E18 along with TCR signaling, resulting in the comparatively low expression levels in SKG mice at E18. This may be similar to the phenotype of thymic CD3^{lo}Vγ5TCR^{lo} cells accumulating in Rank-deficient mice expressing lower Skint-1 (40). SKG mutant mice did not show a change in the expression of CD24 and CD45RB on thymic Vγ5Vδ1$^+$ T cells. Thymocyte development requires multi-step programs executed by many environmental factors (67); *e.g.*, Rank$^{-/-}$ mice show decreased expression of CD45RB as well as decreased numbers of thymic Vγ5$^+$ T cells (40). Lymphotoxin signaling from DP cells is also crucial to induce the expression of γδ-biased genes in γδ T cells (68). Therefore, it is conceivable that these molecules, including Skint1, are involved in the development of Vγ5Vδ1$^+$ T cells in embryonic thymus, to some extent.

We observed that early-life epidermal Vγ5$^+$T cells were round, and dendrites were generated in adult WT and GF, but not in SKG mice. DETC dendrites include γδTCR-containing microclusters that interact with surrounding cells (69). DETCs can generate new dendrites in response to stimuli (66). Based on these reports, we propose that TCR interactions with a ligand are necessary to generate dendrites. However, such a hypothetical DETC TCR ligand in the steady state has not yet been found, except in the case of wounded keratinocytes (70). Hence, more research is necessary to investigate the mechanism. Besides, in SKG mice, migration of early-life

epidermal Vγ5^{+}T cells from the thymus seem to be normal, however we can't exclude the possibility that insufficient TCR signaling in the thymus affects the morphogenesis and proliferation of the T cells in the epidermis except for TCR signaling step.

As in DETCs, Vγ6^{+} γδ T cells originate in the embryonic thymus, and further mature and self-renew in the peripheral organs, leading to body homeostasis; *e.g.*, Vγ6^{+} γδ T cells in adipose tissue are involved in regulation of body core temperature *via* IL-17 production, and in the development of Treg cells (71). On the other hand, intestinal Vγ7^{+} γδ T cells originate in the thymus or in the intestine, and further mature and proliferate around weaning (51). The intestinal γδ T cells induce the expression of genes involved in the absorption and transport of carbohydrates due partly to suppression of IL-22 production (72). It is possible that the extrathymic development of these various γδ T cells and DETCs affect their peripheral functions. Therefore, further work is necessary to elucidate the peripheral selection mechanism(s) of γδ T cells, leading to their ability to maintain host physiology.

Funding

This work was supported by a grant from the Shimizu Foundation for Immunology and Neuroscience in 2020 (to K.T.).

Acknowledgments

K.S. was supported by a Scholarship for Doctoral Students in Immunology from the Japanese Society for Immunology. We thank F. Namai (Shinshu University) for the help with 16S rRNA sequencing.

Authorship

K. Sudo conceived and designed the study, performed most of experiments, interpreted data and wrote the manuscript; T. Todoroki performed experiments; Y. Ka provided germ-free mice; K. Takahara conceived and designed the study, interpreted data and wrote the manuscript, with extensive input from all authors.

Conflict of Interest Policy

The authors declare no competing interests.

Abbreviations

DETC, dendritic epidermal T cell; DN, double-negative; DP, double-positive; E, embryonic day; GF, germ-free; ITAM, immunoreceptor tyrosine-based activation motif; LC, Langerhans cell.

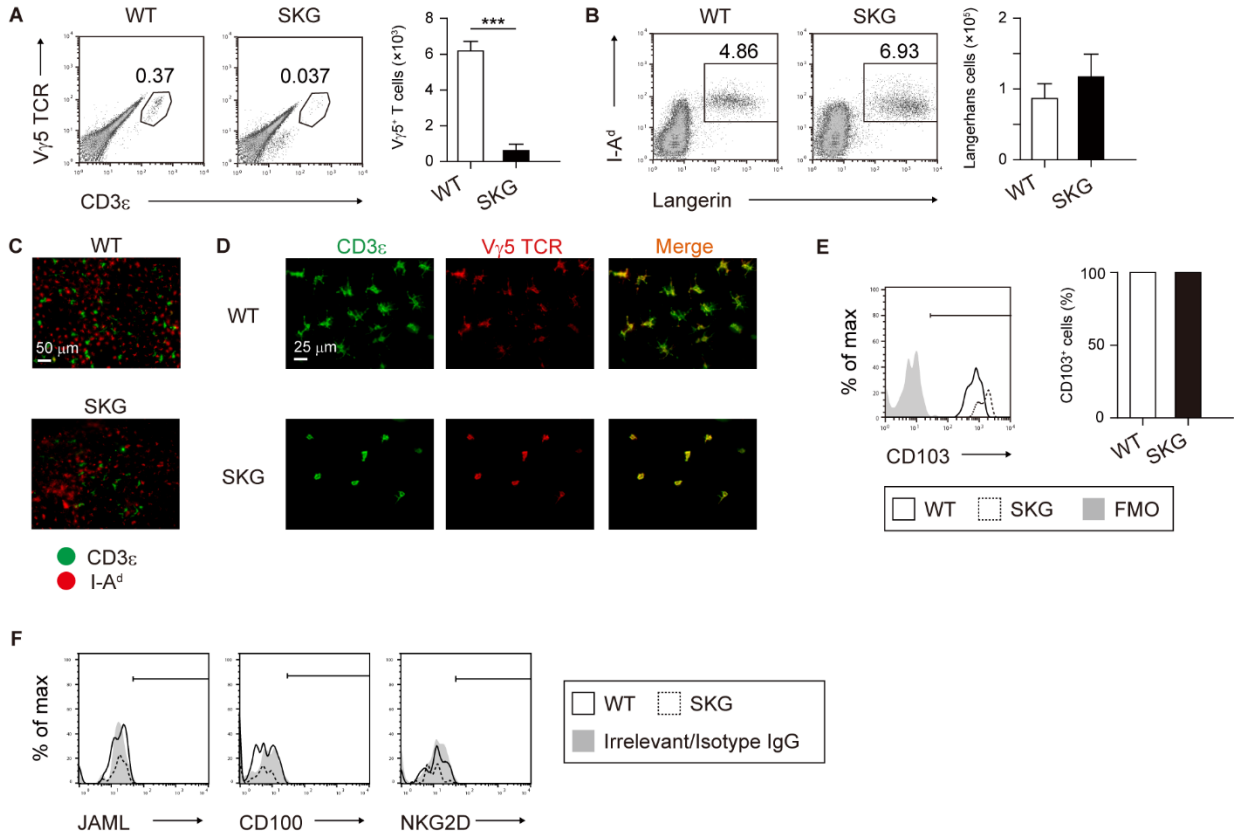

Figure 1. Effect of attenuated TCR signaling on adult epidermal γδ T cells.

(A and B) Flow cytometric analyses of Vγ5$^+$ T cells (A) and Langerhans cells (LCs) (B) in adult WT and SKG mouse ear epidermis. Vγ5$^+$ T cells and LCs were identified as CD3ε$^+$Vγ5TCR$^+$ and I-A^{d+}Langerin$^+$, respectively. Dead cells were excluded by 7-AAD. Cell populations from the left ear were analyzed. These experiments were performed four times, and representative results are shown. ***$p < 0.001$ ($n = 3$). **(C and D)** Immunostaining of ear epidermis. Epidermal sheets from adult WT and SKG mice were stained with anti-CD3ε (green) and anti-I-A^d (red) (C), or anti-CD3ε (green) and anti-Vγ5TCR (red) (D). Scale bar, 50 μm (C) or 25 μm (D). These experiments were performed four times ($n = 3$), and representative results are shown. **(E)** Flow cytometric analyses of CD103 expression on CD3ε$^+$γδTCR^{hi} cells from adult WT and SKG mouse ear epidermis. FMO, fluorescence minus one. These experiments were performed two times ($n = 3$), and representative results are shown. **(F)** Flow cytometric analyses of JAML, CD100 and NKG2D expressions on Vγ5$^+$ T cells from adult WT and SKG mouse ear epidermis. Irrelevant IgG was

used in JAML staining experiments, whereas isotype IgG was used in CD100 and NKG2D staining experiments. These experiments were performed two times (n = 4), and representative results are shown. A two-tailed Student's t-test was used for statistical analyses. All data are expressed as the mean ± S.D.

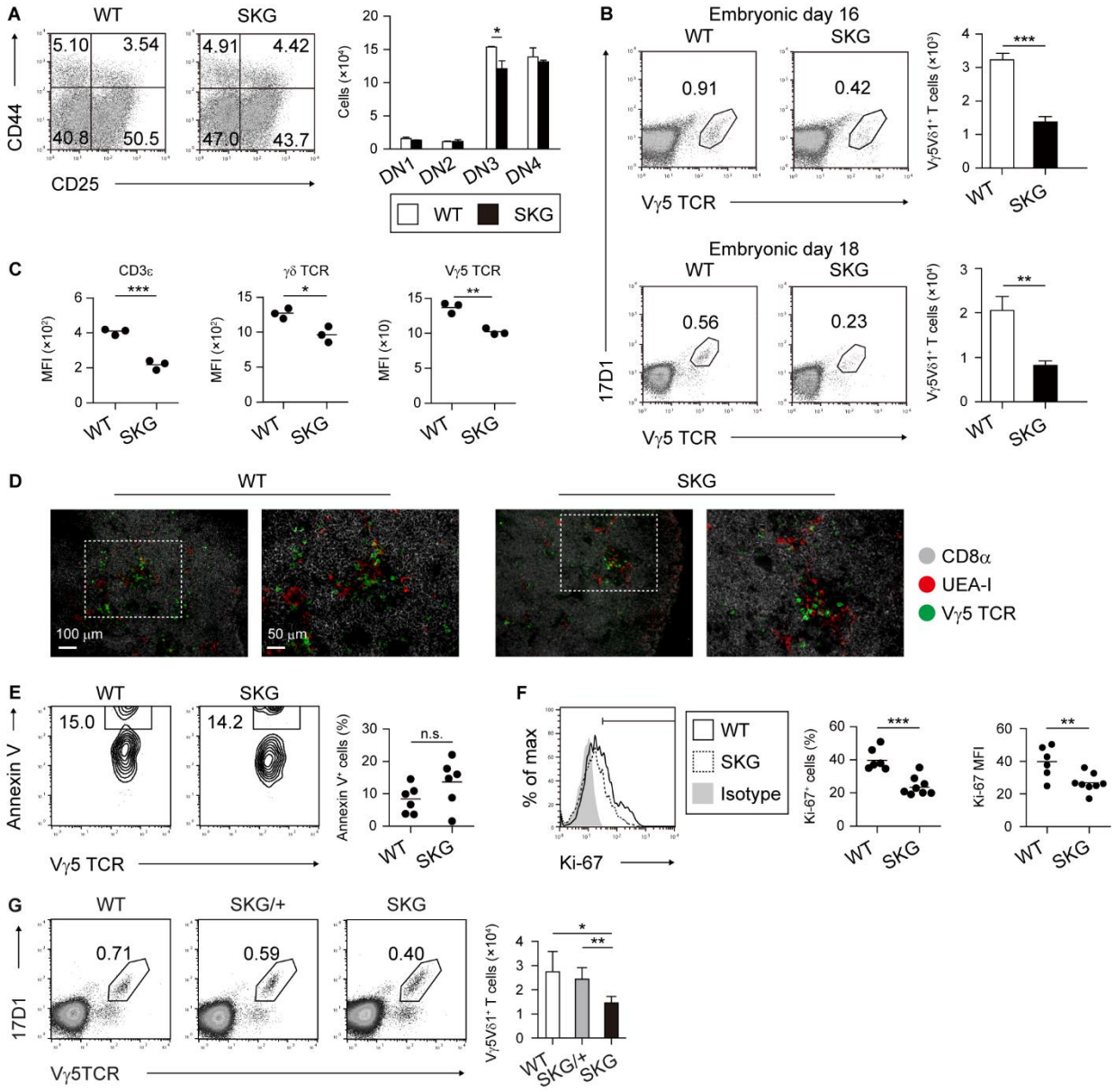

501

502 **Figure 2. Effect of attenuated TCR signaling on fetal thymic Vγ5Vδ1$^+$ T cell development.**

503 **(A)** Flow cytometric analysis of DN1-4 cells in E16 WT and SKG mouse thymus. Each cell is
504 identified as follows: DN1 as Lineage (CD3ε, 4, 8α, 11b, 11c, 45R, Gr-1, Ly6C) (Lin)$^-$
505 CD44$^+$CD25$^-$ cells; DN2 as Lin$^-$CD44$^+$CD25$^+$ cells; DN3 as Lin$^-$CD44$^-$CD25$^+$ cells; DN4 as Lin$^-$
506 CD44$^-$CD25$^-$ cells. These experiments were performed four times, and representative results are
507 shown. *$p < 0.05$ ($n = 3$). **(B)** Flow cytometric analysis of thymic Vγ5Vδ1$^+$ T cells from WT and

SKG mice at E16 (top) and E18 (bottom). Vγ5Vδ1$^+$ T cells were identified by Vγ5TCR$^+$17D1$^+$ expression. These experiments were performed three times, and representative results are shown. $^{**}p < 0.01$, $^{***}p < 0.001$ ($n = 3$). **(C)** Flow cytometric analysis of MFI of CD3ε (left), γδ TCR (middle) and Vγ5 TCR (right) expressed on thymic Vγ5Vδ1$^+$ T cells from E18 WT and SKG mice. Each symbol represents one mouse. These experiments were performed three times, and representative results are shown. $^{*}p < 0.05$, $^{**}p < 0.01$, $^{***}p < 0.001$ ($n = 3$). **(D)** Immunostaining of fetal thymic sections. Sections from E18 WT and SKG mice were stained with anti-CD8α (gray), UEA-I (red) and anti-Vγ5TCR (green). Scale bar, 100 μm (left) and 50 μm (right). These experiments were performed seven times, and representative results are shown ($n = 3$). **(E)** Flow cytometric analysis of Annexin V staining of thymic Vγ5Vδ1$^+$ T cells from E18 WT and SKG mice. Each symbol represents one mouse. These experiments were performed three times, and pooled results from two independent experiments are shown ($n = 6$). n.s., not significant. **(F)** Flow cytometric analysis of Ki-67 expression (left) and MFI (right) in Vγ5Vδ1$^+$ T cells from thymuses of E18 WT and SKG mice. Each symbol represents one mouse. These experiments were performed three times, and pooled results from two independent experiments are shown. $^{**}p < 0.01$, $^{***}p < 0.001$ ($n = 6$-8). **(G)** Flow cytometric analysis of thymic Vγ5Vδ1$^+$ T cells from WT, SKG/+ and SKG mice at E18. These experiments were performed two times, and pooled results from two independent experiments are shown. $^{*}p < 0.05$, $^{**}p < 0.01$ ($n = 4$-8). A two-tailed Student's *t*-test was used for statistical analyses. All data are expressed as the mean ± S.D.

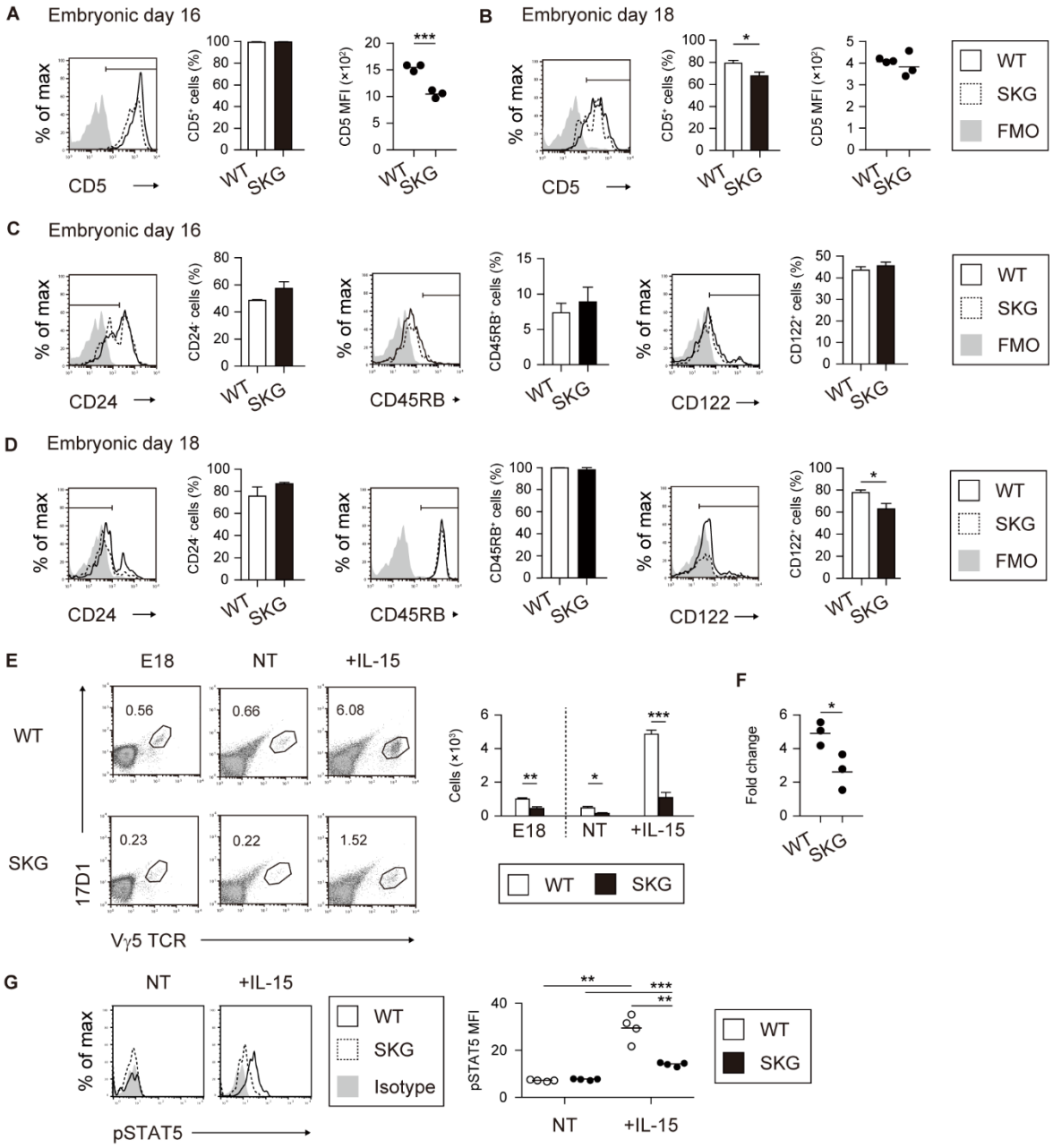

528

529 **Figure 3. Maturation of Vγ5Vδ1⁺ T cells is impaired by attenuated TCR signaling.**

530 **(A and B)** Flow cytometric analysis of CD5 expression on Vγ5Vδ1⁺ T cells from WT and SKG
531 mouse thymus at E16 (A) and E18 (B). Each symbol represents one mouse. These experiments
532 were performed two times, and representative results are shown. *$p < 0.05$, ***$p < 0.001$ ($n = 3$).
533 **(C and D)** Flow cytometric analysis of CD24 (left panel), CD45RB (middle panel), and CD122

(right panel) expression on Vγ5Vδ1$^+$ T cells from WT and SKG mouse thymus at E16 (C) and E18 (D), respectively. These experiments were performed two times, and representative results are shown. *$p < 0.05$ ($n = 3$). **(E)** Flow cytometric analysis of Vγ5Vδ1$^+$ T cells in cultured medium. Fetal thymocytes from E18 WT and SKG mice were cultured with or without 50 ng/ml IL-15 for 48 hours. The number of Vγ5Vδ1$^+$ T cells at E18 was calculated by multiplying the frequency by 2×10^5 thymocytes. **(F)** Fold change showing the ratio of the number of Vγ5Vδ1$^+$ T cells in the IL-15-treated group over the number of E18 thymic Vγ5Vδ1$^+$ T cells per 2×10^5 thymocytes in (E). Each symbol represents one mouse. **(E and F)** These experiments were performed two times, and representative results are shown. *$p < 0.05$, **$p < 0.01$, ***$p < 0.001$ ($n = 3$). **(G)** Flow cytometric analysis of STAT5 phosphorylation in Vγ5Vδ1$^+$ T cells from WT and SKG mouse thymus at E18. After cell surface marker staining, thymocytes were treated with 50 ng/mL IL-15 for 15 min at 37ºC. The cells were then stained with anti-pSTAT5 antibody following fixation and permeabilization. Each symbol represents one mouse. These experiments were performed two times, and representative results are shown. **$p < 0.01$, ***$p < 0.001$ ($n = 4$). A two-tailed Student's *t*-test was used for statistical analyses. All data are expressed as the mean ± S.D.

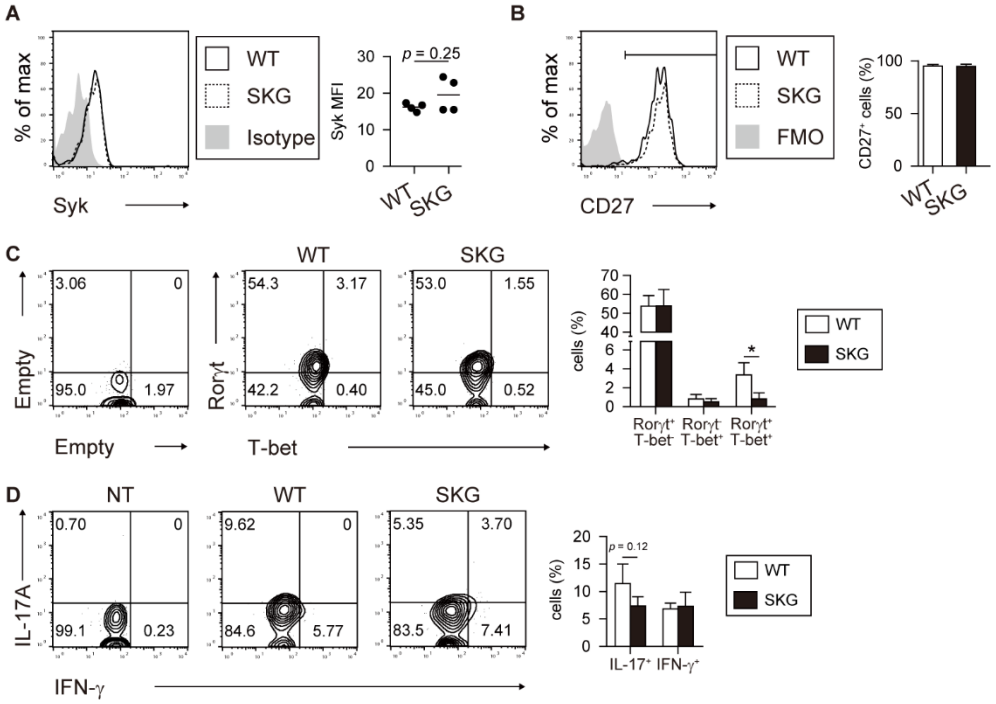

Figure 4. Effect of attenuated TCR signaling on cytokine production of Vγ5Vδ1$^+$ T cells.

(A) Flow cytometric analysis of Syk expression in Vγ5Vδ1$^+$ T cells from WT and SKG mouse thymus at E18. Each symbol represents one mouse. These experiments were performed two times, and representative results are shown (n = 4). n.s., not significant. **(B)** Flow cytometric analysis of CD27 expression on Vγ5Vδ1$^+$ T cells from WT and SKG mouse thymus at E18. These experiments were performed two times, and representative results are shown (n = 4). **(C)** Flow cytometric analysis of Rorγt and T-bet expression in Vγ5Vδ1$^+$ T cells from WT and SKG mouse thymus at E18. These experiments were performed two times, and representative results are shown. *$p < 0.05$ (n = 4). **(D)** Flow cytometric analysis of IL-17A and IFN-γ production in Vγ5Vδ1$^+$ T cells from WT and SKG mouse thymus at E18. Thymocytes were stimulated with 25 ng/ml PMA, 1 μg/ml ionomycin and GolgiPlug (1 : 1000) for 4 hr. These experiments were performed two times, and representative results are shown. *$p < 0.05$ (n = 4).

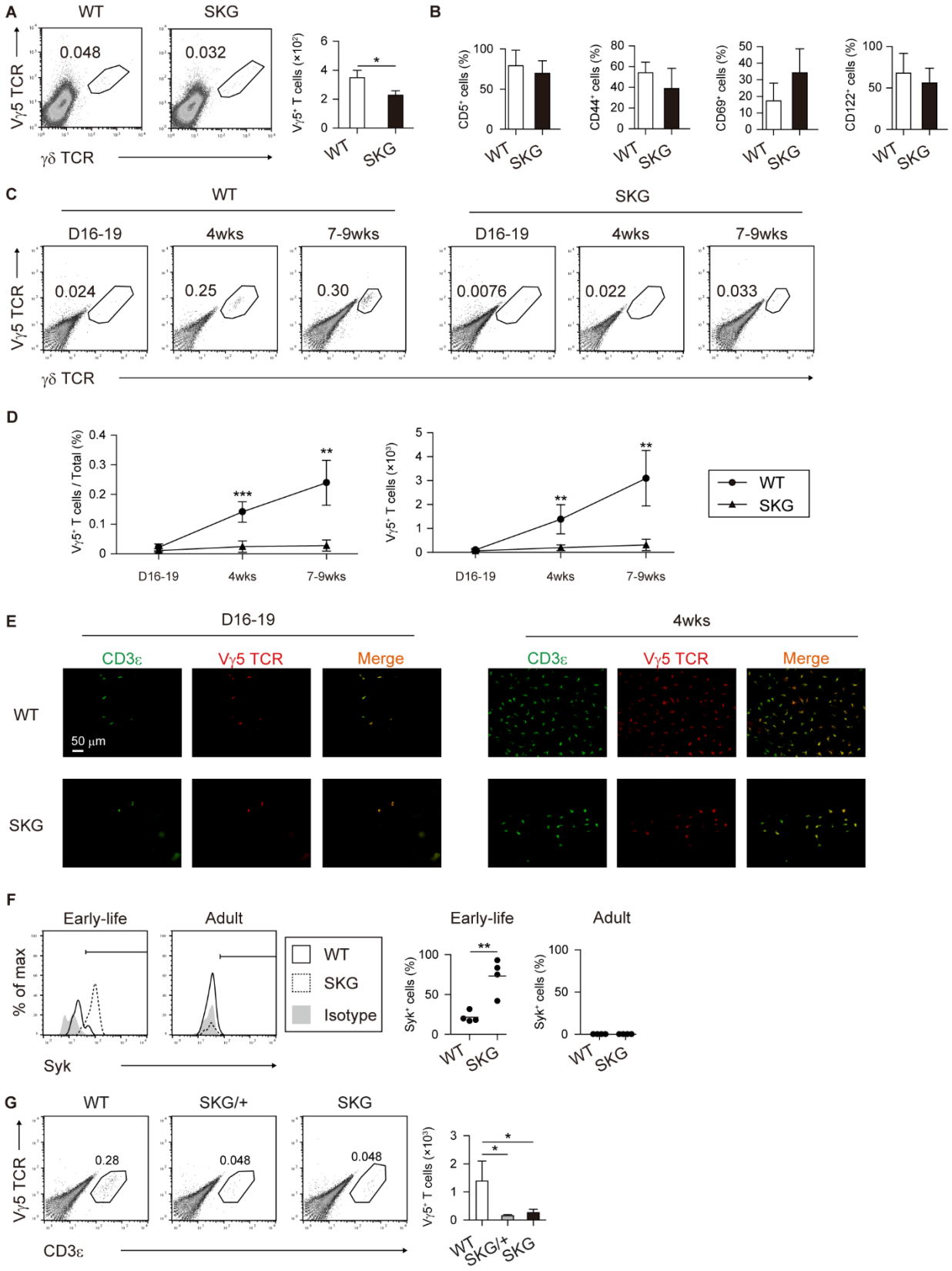
A
WT
SKG
0.048
0.032
Vγ5 TCR
γδ TCR
Vγ5⁺ T cells (×10²)
WT
SKG
B
CD5⁺ cells (%)
CD44⁺ cells (%)
CD69⁺ cells (%)
CD122⁺ cells (%)
C
WT
SKG
D16-19
4wks
7-9wks
0.024
0.25
0.30
0.0076
0.022
0.033
D
Vγ5⁺ T cells / Total (%)
Vγ5⁺ T cells (×10³)
WT
SKG
E
D16-19
4wks
CD3ε
Vγ5 TCR
Merge
50 μm
F
Early-life
Adult
% of max
Syk
Isotype
Syk⁺ cells (%)
G
SKG/+
0.28
0.048

Figure 5. Effect of attenuated TCR signaling on early-life epidermal Vγ5$^+$ T cell proliferation.

(A) Flow cytometric analysis of Vγ5$^+$ T cells from ear epidermis in WT and SKG mice at age 16-19-days. Dead cells were excluded by 7AAD. Cell populations from both the right and left ears were analyzed. These experiments were performed five times, and representative results are shown. *$p < 0.05$ ($n = 3$). **(B)** Flow cytometric analysis of CD5 (far left), CD44 (left), CD69 (right) and CD122 (far right) expression on Vγ5$^+$ T cells from 16-19-day-old WT and SKG mouse ear epidermis. Dead cells were excluded by 7AAD. These experiments were performed four times and representative results are shown ($n = 3$). **(C and D)** Flow cytometric analysis of Vγ5$^+$ T cells in WT and SKG mouse ear epidermis at indicated times. Dead cells were excluded by 7AAD. Cell populations from the left ear were analyzed. These experiments were performed four times, and pooled results from two independent experiments are shown ($n = 6$-7). Statistical analysis was performed between age-matched WT and SKG mice. **$p < 0.01$, ***$p < 0.001$. **(E)** Immunostaining of ear epidermis. Epidermal sheets from WT (top panels) and SKG mice (bottom panels) at age 16-19-days (left panels) and 4-weeks (right panels), were stained with anti-CD3ε (green) and anti-Vγ5TCR (red). Scale bar, 50 μm. These experiments were performed four times, and representative results are shown ($n = 3$). **(F)** Flow cytometric analysis of Syk expression in Vγ5$^+$ T cells from ear epidermis in WT and SKG mice at the indicated times. Each symbol represents one mouse. Dead cells were excluded by 7AAD. These experiments were performed two times, and representative results are shown ($n = 4$). **$p < 0.01$. **(G)** Flow cytometric analysis of Vγ5$^+$ T cells from ear epidermis in adult WT, SKG/+ and SKG mice. Dead cells were excluded by 7AAD. Cell populations from the left ear were analyzed. These experiments were performed two times, and representative results are shown. *$p < 0.05$ ($n = 3$-6). A two-tailed Student's *t*-test was used for statistical analyses. All data are expressed as the mean ± S.D.

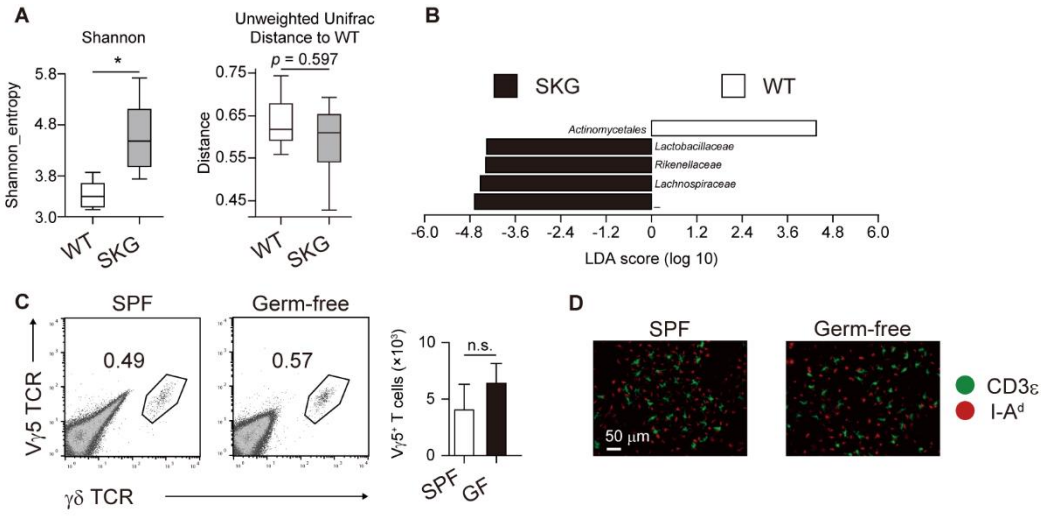

Figure 6. DETC proliferation is independent of skin microbiota.

(A) Alpha-diversity and beta-diversity analyses of skin microbiota from adult WT and SKG mouse ears. The diversities were calculated with a Shannon index (left) and unweighted UniFrac (right), respectively. These experiments were performed two times, and pooled results from two independent experiments are shown. *$p < 0.05$ ($n = 4$). **(B)** LDA score of skin microbiota at the family level from adult WT and SKG mouse ears. The LDA score was calculated with LEfSe, and the only scores in which the p value was less than 0.05 are shown. These experiments were performed two times, and pooled results from two independent experiments are shown ($n = 4$). **(C)** Flow cytometric analysis of ear epidermal $V\gamma5^+$ T cells in adult SPF and Germ-free (GF) mice. Dead cells were excluded by 7AAD. Cell populations from the left ear were analyzed. These experiments were performed three times, and representative results are shown ($n = 3$). n.s., not significant. **(D)** Immunostaining of ear epidermis. Epidermal sheets of adult SPF and GF mice were stained with anti-CD3ε (green) and anti-I-A^d (red). Scale bar, 50 μm. These experiments were performed three times, and representative results are shown ($n = 3$). A two-tailed Student's t-test was used for statistical analyses. A Kruskal-Wallis test was used in (A). A Kruskal-Wallis test and a pairwise Wilcoxon test was used in (B). All data are expressed as the mean ± S.D.

References

1 Hayday, A., Saito, H., Gillies, S., *et al*. 1985. Structure, organization, and somatic rearrangement of T cell gamma genes. *Cell* 40:259.

2 Garman, R., Doherty, P., and Raulet, D. 1986. Diversity, rearrangement, and expression of murine T cell gamma genes. *Cell* 45:733.

3 Heilig, J. S. and Tonegawa, S. 1986. Diversity of murine gamma genes and expression in fetal and adult T lymphocytes. *Nature* 322:836.

4 Vantourout, P. and Hayday, A. 2013. Six-of-the-best: unique contributions of γδ T cells to immunology. *Nat. Rev. Immunol.* 13:88.

5 Girardi, M., Oppenheim, D. E., Steele, C. R., *et al*. 2001. Regulation of cutaneous malignancy by γδ T cells. *Science* 294:605.

6 Jameson, J., Ugarte, K., Chen, N., *et al*. 2002. A role for skin γδ T cells in wound repair. *Science* 296:747.

7 Strid, J., Roberts, S. J., Filler, R. B., *et al*. 2008. Acute upregulation of an NKG2D ligand promotes rapid reorganization of a local immune compartment with pleiotropic effects on carcinogenesis. *Nat. Immunol.* 9:146.

8 Nielsen, M. M., Witherden, D. A., and Havran, W. L. 2017. γδ T cells in homeostasis and host defence of epithelial barrier tissues. *Nat. Rev. Immunol.* 17:733.

9 Crawford, G., Hayes, M., Seoane, R., *et al*. 2018. Epithelial damage and tissue γδ T cells promote a unique tumor-protective IgE response. *Nat. Immunol.* 19:859.

10 Havran, W. L. and Allison, J. P. 1988. Developmentally ordered appearance of thymocytes expressing different T-cell antigen receptors. *Nature* 335:443.

11 Havran, W. and Allison, J. 1990. Origin of Thy-1^+ dendritic epidermal cells of adult mice from fetal thymic precursors. *Nature* 344:68.

12 Boyden, L. M., Lewis, J. M., Barbee, S. D., *et al*. 2008. Skint1, the prototype of a newly identified immunoglobulin superfamily gene cluster, positively selects epidermal γδ T cells. *Nat. Genet.* 40:656.

13 Elbe, A., Tschachler, E., Steiner, G., *et al*. 1989. Maturational steps of bone marrow-derived dendritic murine epidermal cells. Phenotypic and functional studies on

Langerhans cells and Thy-1^+ dendritic epidermal cells in the perinatal period. *J. Immunol.* 143:2431.

14 Correa, I., Bix, M., Liao, N., *et al*. 1992. Most γδ T cells develop normally in β_2-microglobulin-deficient mice. *Proc. Natl. Acad. Sci. U. S. A.* 89:653.

15 Bigby, M., Markowitz, J., Bleicher, P., *et al*. 1993. Most γδ T cells develop normally in the absence of MHC class II molecules. *J. Immunol.* 151:4465.

16 Xiong, N., Kang, C., and Raulet, D. H. 2004. Positive selection of dendritic epidermal γδ T cell precursors in the fetal thymus determines expression of skin-homing receptors. *Immunity* 21:121.

17 Mallick-Wood, C. A., Lewis, J. M., Richie, L. I., *et al*. 1998. Conservation of T cell receptor conformation in epidermal γδ cells with disrupted primary Vγ gene usage. *Science* 279:1729.

18 Hara, H., Kishihara, K., Matsuzaki, G., *et al*. 2000. Development of dendritic epidermal T cells with a skewed diversity of γδTCRs in Vδ1-deficient mice. *J. Immunol.* 165:3695.

19 Kadlecek, T. A., van Oers, N. S., Lefrancois, L., *et al*. 1998. Differential requirements for ZAP-70 in TCR signaling and T cell development. *J. Immunol.* 161:4688.

20 Endo, Y., Ishikawa, O., and Negishi, I. 2005. Zeta-chain-associated protein-70 molecule is essential for the proliferation and the final maturation of dendritic epidermal T cells. *Exp. Dermatol.* 14:188.

21 Muro, R., Nitta, T., Nakano, K., *et al*. 2018. γδTCR recruits the Syk/PI3K axis to drive proinflammatory differentiation program. *J. Clin. Invest.* 128:415.

22 Lewis, J. M., Girardi, M., Roberts, S. J., *et al*. 2006. Selection of the cutaneous intraepithelial $\gamma\delta^+$ T cell repertoire by a thymic stromal determinant. *Nat. Immunol.* 7:843.

23 Turchinovich, G. and Hayday, A. C. 2011. Skint-1 identifies a common molecular mechanism for the development of interferon-gamma-secreting versus interleukin-17-secreting gammadelta T cells. *Immunity* 35:59.

24 Noraz, N., Schwarz, K., Steinberg, M., *et al*. 2000. Alternative antigen receptor (TCR) signaling in T cells derived from ZAP-70-deficient patients expressing high levels of Syk. *J. Biol. Chem.* 275:15832.

25 Gelfand, E., Weinberg, K., Mazer, B., *et al*. 1995. Absence of ZAP-70 prevents signaling through the antigen receptor on peripheral blood T cells but not on thymocytes. *J. Exp. Med.* 182:1057.

26 Toyabe, S., Watanabe, A., Harada, W., *et al*. 2001. Specific immunoglobulin E responses in ZAP-70-deficient patients are mediated by Syk-dependent T-cell receptor signalling. *Immunology* 103:164.

27 Enyedy, E., Nambiar, M., Liossis, S., *et al*. 2001. Fcε receptor type I γ chain replaces the deficient T cell receptor ζ chain in T cells of patients with systemic lupus erythematosus. *Arthritis Rheum.* 44:1114.

28 Krishnan, S., Juang, Y., Chowdhury, B., *et al*. 2008. Differential expression and molecular associations of Syk in systemic lupus erythematosus T cells. *J. Immunol.* 181:8145.

29 Sakaguchi, N., Takahashi, T., Hata, H., *et al*. 2003. Altered thymic T-cell selection due to a mutation of the ZAP-70 gene causes autoimmune arthritis in mice. *Nature* 426:454.

30 Wencker, M., Turchinovich, G., Di Marco Barros, R., *et al*. 2014. Innate-like T cells straddle innate and adaptive immunity by altering antigen-receptor responsiveness. *Nat. Immunol.* 15:80.

31 Bolyen, E., Rideout, J., Dillon, M., *et al*. 2019. Reproducible, interactive, scalable and extensible microbiome data science using QIIME 2. *Nat. Biotechnol.* 37:852.

32 Segata, N., Izard, J., Waldron, L., *et al*. 2011. Metagenomic biomarker discovery and explanation. *Genome Biol.* 12:R60.

33 Caux, C., Massacrier, C., Dubois, B., *et al*. 1999. Respective involvement of TGF-β and IL-4 in the development of Langerhans cells and non-Langerhans dendritic cells from $CD34^+$ progenitors. *J. Leukoc. Biol.* 66:781.

34 Schlickum, S., Sennefelder, H., Friedrich, M., *et al*. 2008. Integrin α_E(CD103)β7 influences cellular shape and motility in a ligand-dependent fashion. *Blood* 112:619.

35 Witherden, D., Verdino, P., Rieder, S., *et al*. 2010. The Junctional Adhesion Molecule JAML Is a Costimulatory Receptor for Epithelial γδ T Cell Activation. *Science* 329:1205.

36 Whang, M., Guerra, N., and Raulet, D. 2009. Costimulation of dendritic epidermal γδ T cells by a new NKG2D ligand expressed specifically in the skin. *J. Immunol.* 182:4557.

37 Witherden, D., Watanabe, M., Garijo, O., *et al*. 2012. The CD100 Receptor Interacts With Its Plexin B2 Ligand to Regulate Epidermal γδ T Cell Function. *Immunity* 37:314.

38 Jameson, J. M., Cauvi, G., Witherden, D. A., and Havran, W. L. 2004. A keratinocyte-responsive γδ TCR is necessary for dendritic epidermal T cell activation by damaged keratinocytes and maintenance in the epidermis. *J. Immunol.* 172:3573.

39 Mallick-Wood, C. A., Pao, W., Cheng, A. M., *et al*. 1996. Disruption of epithelial γδ T cell repertoires by mutation of the Syk tyrosine kinase. *Proc. Natl. Acad. Sci. U. S. A.* 93:9704.

40 Roberts, N. A., White, A. J., Jenkinson, W. E., *et al*. 2012. Rank signaling links the development of invariant γδ T cell progenitors and Aire^{+} medullary epithelium. *Immunity* 36:427.

41 Takaba, H. and Takayanagi, H. 2017. The mechanisms of T cell selection in the Thymus. *Trends Immunol.* 38:805.

42 Takeuchi, Y., Hirota, K., and Sakaguchi, S. 2020. Impaired T cell receptor signaling and development of T cell-mediated autoimmune arthritis. *Immunol. Rev.* 294:164.

43 Azzam, H. S., Grinberg, A., Lui, K., *et al*. 1998. CD5 expression is developmentally regulated by T cell receptor (TCR) signals and TCR avidity. *J. Exp. Med.* 188:2301.

44 Leclercq, G., Plum, J., Nandi, D., *et al*. 1993. Intrathymic differentiation of Vγ3 T cells. *J. Exp. Med.* 178:309.

45 Taniguchi, T. and Minami, Y. 1993. The IL-2/IL-2 receptor system: a current overview. *Cell* 73:5.

46 Kawai, K., Suzuki, H., Tomiyama, K., *et al*. 1998. Requirement of the IL-2 receptor β chain for the development of Vγ3 dendritic epidermal T cells. *J. Invest. Dermatol.* 110:961.

47 De Creus, A., Van Beneden, K., Stevenaert, F., *et al*. 2002. Developmental and functional defects of thymic and epidermal Vγ3 cells in IL-15-deficient and IFN regulatory factor-1-deficient mice. *J. Immunol.* 168:6486.

48 Johnston, J., Bacon, C., Finbloom, D., *et al*. 1995. Tyrosine phosphorylation and activation of STAT5, STAT3, and Janus kinases by interleukins 2 and 15. *Proc. Natl. Acad. Sci. U. S. A.* 92:8705.

744 49 Ribot, J. C., deBarros, A., Pang, D. J., *et al*. 2009. CD27 is a thymic determinant of the
745 balance between interferon-gamma- and interleukin 17-producing gammadelta T cell
746 subsets. *Nat. Immunol.* 10:427.
747 50 Ivanov, I., McKenzie, B., Zhou, L., *et al*. 2006. The orphan nuclear receptor RORγt
748 directs the differentiation program of proinflammatory IL-17^{+} T helper cells. *Cell*
749 126:1121.
750 51 Di Marco Barros, R., Roberts, N. A., Dart, R. J., Vantourout, P., *et al*. 2016. Epithelia
751 Use Butyrophilin-like Molecules to Shape Organ-Specific γδ T Cell Compartments. *Cell*
752 167:203.
753 52 Tanaka, S., Maeda, S., Hashimoto, M., *et al*. 2010. Graded attenuation of TCR signaling
754 elicits distinct autoimmune diseases by altering thymic T cell selection and regulatory T
755 cell function. *J. Immunol.* 185:2295.
756 53 Yoshitomi, H., Sakaguchi, N., Kobayashi, K., *et al*. 2005. A role for fungal {beta}-
757 glucans and their receptor Dectin-1 in the induction of autoimmune arthritis in genetically
758 susceptible mice. *J. Exp. Med.* 201:949.
759 54 Rehaume, L., Mondot, S., Aguirre de Cárcer, D., *et al*. 2014. ZAP-70 genotype disrupts
760 the relationship between microbiota and host, leading to spondyloarthritis and ileitis in
761 SKG mice. *Arthritis Rheumatol.* 66:2780.
762 55 Naik, S., Bouladoux, N., Wilhelm, C., *et al*. 2012. Compartmentalized control of skin
763 immunity by resident commensals. *Science* 337:1115.
764 56 Constantinides, M., Link, V., Tamoutounour, S., *et al*. 2019. MAIT cells are imprinted by
765 the microbiota in early life and promote tissue repair. *Science* 366.
766 57 Chan, A., van Oers, N., Tran, A., *et al*. 1994. Differential expression of ZAP-70 and Syk
767 protein tyrosine kinases, and the role of this family of protein tyrosine kinases in TCR
768 signaling. *J. Immunol.* 152:4758.
769 58 Cheng, A., Rowley, B., Pao, W., *et al*. 1995. Syk tyrosine kinase required for mouse
770 viability and B-cell development. *Nature* 378:303.
771 59 Turner, M., Mee, P. J., Costello, P. S., *et al*. 1995. Perinatal lethality and blocked B-cell
772 development in mice lacking the tyrosine kinase Syk. *Nature* 378:298.
773 60 Negishi, I., Motoyama, N., Nakayama, K., *et al*. 1995. Essential role for ZAP-70 in both
774 positive and negative selection of thymocytes. *Nature* 376:435.

61 Cheng, A., Negishi, I., Anderson, S., *et al*. 1997. The Syk and ZAP-70 SH2-containing tyrosine kinases are implicated in pre-T cell receptor signaling. *Proc. Natl. Acad. Sci. U. S. A.* 94:9797.

62 Gong, Q., White, L., Johnson, R., *et al*. 1997. Restoration of thymocyte development and function in zap-$70^{-/-}$ mice by the Syk protein tyrosine kinase. *Immunity* 7:369.

63 de Jong, M., Vriend, L., Theelen, B., *et al*. 2010. C-type lectin Langerin is a β-glucan receptor on human Langerhans cells that recognizes opportunistic and pathogenic fungi. *Mol. Immunol.* 47:1216.

64 van Dalen, R., De La Cruz Diaz, J., Rumpret, M., *et al*. 2019. Langerhans Cells Sense Staphylococcus aureus Wall Teichoic Acid through Langerin To Induce Inflammatory Responses. *mBio* 10:e00330.

65 de Witte, L., Nabatov, A., Pion, M., *et al*. 2007. Langerin is a natural barrier to HIV-1 transmission by Langerhans cells. *Nat. Med.* 13:367.

66 Chodaczek, G., Papanna, V., Zal, M. A., and Zal, T. 2012. Body-barrier surveillance by epidermal γδ TCRs. *Nat. Immunol.* 13:272.

67 Hosokawa, H. and Rothenberg, E. 2020. How transcription factors drive choice of the T cell fate. *Nat. Rev. Immunol.* 21:162.

68 Silva-Santos, B., Pennington, D. J., and Hayday, A. C. 2005. Lymphotoxin-mediated regulation of γδ cell differentiation by αβ T cell progenitors. *Science* 307:925.

69 Chodaczek, G., Toporkiewicz, M., Zal, M., and Zal, T. 2018. Epidermal T Cell Dendrites Serve as Conduits for Bidirectional Trafficking of Granular Cargo. *Front. Immunol.* 9.

70 Komori, H. K., Witherden, D. A., Kelly, R., *et al*. 2012. Cutting edge: dendritic epidermal γδ T cell ligands are rapidly and locally expressed by keratinocytes following cutaneous wounding. *J. Immunol.* 188:2972.

71 Kohlgruber, A., Gal-Oz, S., LaMarche, N., *et al*. 2018. γδ T cells producing interleukin-17A regulate adipose regulatory T cell homeostasis and thermogenesis. *Nat. Immunol.* 19:464.

72 Sullivan, Z. A., Khoury-Hanold, W., Lim, J., *et al*. 2021. γδ T cells regulate the intestinal response to nutrient sensing. *Science* 371.